Available online at www.sciencedirect.com
SCIENCE DIRECT
Journal of Photochemistry and Photobiology A: Chemistry 181 (2006) 19–27
Journal of Photochemistry and Photobiology A:Chemistry
www.elsevier.com/locate/jphotochem

Kinetics studies of methyl methacrylate photopolymerization initiated by titanium dioxide semiconductor nanoparticles

Xiuyuan Ni *, Jing Ye, Ceng Dong

Department of Macromolecular Science, The Key Laboratory of Molecular Engineering of Polymer, State Educational Minister, Fudan University, Shanghai 200433, PR China

Received 8 November 2004; received in revised form 28 September 2005; accepted 18 October 2005
Available online 28 November 2005

Abstract

Kinetics of the photopolymerization of methyl methacrylate (MMA) initiated by TiO_2 nanoparticles in aqueous suspensions was studied. The kinetics equation was established on basis of free radical chain mechanism. The observed dependences of polymerization rate on the variables of the concentration of TiO_2 and the incident light intensity complied with the predictions from the kinetics equation. It was found that the polymerization rate as well as the number-average molecular weight of the synthetic polymers increased rapidly with increasing concentration of monomer. This phenomenon was explained by introducing a model of surface chain propagation. The effect of mass transfer was incorporated through addition of a diffusion flux term to the mass equilibrium of monomer. The initiation quantum efficiency was found to decrease with increasing incident light intensity. pH effects on the photopolymerization were investigated exclusively in this study. It was found that the rate of polymerization was pH dependent, while the configuration of polymer remains unchanged. The results from ESR spin-trapping analysis at various pH conditions suggested that trapping holes by OH^- act as a competitive way towards OH radicals. With aids of these results, pH dependence of the initiation quantum efficiency was correlated to the influences of pH on the initiating species. Assuming that the photogenerated holes have higher initiation efficiency than OH radicals, the observed pH dependence of polymerization rate can be reasonably interpreted.

Keywords: Photopolymerization; Semiconductor nanoparticles; Titanium dioxide; Kinetics; Free radical mechanism

1. Introduction

Work in the field of photopolymerizations has acquired important progresses in the aspects such as visible-light excitations, cationic polymerization and kinetics simulations of great value [1–3]. Polymerizations of vinyl monomers can also be initiated with semiconductors excited by ultraviolet irradiations [4–6]. Pioneering contributions have been made by the authors addressing the photopolymerizations using colloidal semiconductors as initiators [7–10]. Initiators such as quantum-sized CdS, ZnO and TiO_2 colloids were applied to polymerizations of vinyl monomers in non-aqueous solvents or monomer bulk. Processes of these polymerizations have been shown to associate with the chemical nature of semiconductors, particle sizes and organic photo-sensitizers added.

Using semiconductor nanoparticles to initiate polymerization provides a new pathway to polymer/inorganic nanocomposite, while the in situ polymerization can produce a composite composed of polymers and highly dispersed nanoparticles [10,11]. In a previous work, we have observed the morphology of TiO_2 nanoparticles encircled by photogenerated polymers [11]. Recently, semiconductor nanoparticles as fillers have been proved to improve electrical properties of polymer materials [12]. It appears that this photopolymerization have a good future in preparing polymer based conductive materials. The interface effects of interests are strongly expected from the direct participation of the particles into the polymerization. The visible-light photocatalysis of TiO_2 materials has been reported [13], from which follows that solar curing water-borne coatings are possible. As known, the building coatings and other water-borne coatings suffer from a low rate of solidification. Conventional photo-cured coatings employ organic sensitizers, and are always cured by powerful irradiations. Photopolymerizations by nanosized semiconductors, as

* Corresponding author. Fax: +86 21 65640293.
E-mail address: xyni@fudan.edu.cn (X. Ni).

1010-6030/$ – see front matter © 2005 Elsevier B.V. All rights reserved.
doi:10.1016/j.jphotochem.2005.10.021

a young and promising technology, are worthy of being studied thoroughly.

This paper represents the results of kinetics studies of the photopolymerization of methyl methacrylate initiated by TiO_2 semiconductor nanoparticles dispersed in aqueous suspensions TiO_2. Commercial Degussa P25 TiO_2 was employed. Due to an advantage by utilization of particle semiconductors in the aspect of polymer purifications [7], properties of the synthetic polymers can be determined without interventions of remained semiconductors in the measurements. These can provide insight into the photocatalytic dependent polymer structures of interest. Experiments of this study were carried out with respects of effects of monomer concentration, light intensity, initiator concentration and pH of the system, with the goal of obtaining a better understanding of this polymerization, and thus acquiring a knowledge of controlling the polymerization and structures of the polymers.

It has been demonstrated in the literature that changing pH of photocatalytic systems varies electrostatic properties of the surface of semiconductor nanoparticles and also shifts the potential of some redox reaction [14]. Effects of pH on the photopolymerizations with semiconductors are a subject of great interest because they can provide insight into the pH dependence of semiconductor photocatalysis in terms of polymerization. In this work, pH effects on the photopolymerization were exclusively investigated. With aids of ESR spin-trapping experiments, pH dependence of polymerization rate was correlated to pH influences on initiating species, and pathways to producing OH radicals in this system were also discussed.

2. Experimental

2.1. Materials

The nano-TiO_2 semiconductors used was Degussa P25 (80% anatase and 20% rutile) with an average diameter of 21 nm and a BET surface area of 50 m^2/g. The structural information was supplied by Degussa Company. All the chemicals used were of analytical reagent grade. Methyl methacrylate (MMA) was distilled before use. Acetone, methanol, hexane and toluene were used as received without further purification. Deionized water was employed in experiments.

2.2. Polymerization

TiO_2 powders were dispersed into aqueous solutions of MMA using the ultrasonic dispersion technique. The feed concentrations of monomer were lower than its solubility in water at the reaction temperature. pH value of the mixture without adjusting was measured to be 4.5. The mixture of 120 ml was moved into a quartz reactor which was equipped with a magnetic stirrer and a water jacket (the thickness is 0.5 cm) connected to a circulator of $CuSO_4$ solution. The internal dimensions of the reactor in column are ϕ 6 cm × 8 cm. UV irradiation towards the reactor was carried out using a mercury vapor lamp, characterized by two chief peaks at 254 and 365 nm in its emission spectrum. The mixture can avoid being irradiated by the rays exclusive of 365 nm, due to the cutting off of $CuSO_4$ solution [11].

The light intensity was controlled by changing the distance between the lamp and the reactor, and was measured by radiometry (UV-A, BJNU photoelectrical Co.). The light pathlength from the lamp to the center of the reactor is adjusted between 13 and 25 cm. It was determined that while the intensity at the reactor position was 13 mW/cm^2 for 365 nm, the light intensity at 254 nm was only 0.085 mW/cm^2. The reaction temperature is at 40 °C. We adjust pH of the reaction system by adding a sodium hydroxide solution.

The raw products were obtained by centrifugation of the reacted mixture, washed by water and then dried under vacuum to remove monomer traces. Acetone was employed to dissolve PMMA contained in the powders, followed by centrifugation to remove TiO_2 particles from the solution. PMMA dissolved in acetone were precipitated into methanol to get pure polymer. TGA tool was used to check the complete purification of the polymer.

2.3. Characterization

The progress of polymerization was monitored by extraction-gas chromatograph (GC) method that has been described in a previous paper [11]. HP Aligent 6890 GC equipped with FID was used for composition measurements of the extract layer. This method has been proved to be an accurate tool for determining MMA concentration in the mixture [11]. The polymerization rate R_p is determined by measuring the change of MMA concentration during the reaction time of 10 min.

Polymer molecular weights (MW) were determined by GPC (HP Aligent 1100) with THF as solvent and calibrated by standard polystyrene. NMR spectra were recorded on a Bruke DMX500 spectrometer at 300 K with $CDCl_3$ as solvent. ESR analysis was carried out with a bruker ER-200 EPR spectrometer using DMPO as a spin trap. The reaction of DMPO and OH radical is as shown by Reaction (1) [15].

In order to determine the polymer yield, TGA were recorded on a Perkin-Elmer Pyris 1 DSC Instrument. The samples tested are of the raw products without further purification (TiO_2 particles were not removed). The reacting system after certain reaction time is subjected to an ultracentrifugation, and a transparent upper layer was obtained. The chemical composition of the layer was determined using a gas chromatograph combined with mass spectrum (GC/MS, Finnigan Voyager).

3. Results and discussion

3.1. Kinetics model of polymerization

3.1.1. Proof of polymerization

Fig. 1 shows the TGA curve of the raw product prepared under the conditions as described in the figure caption. As mentioned in Section 2.3, the sample tested was separated from the reacted mixture by centrifugation and thus consists of TiO_2 particles and PMMA. The constant weight-loss depicted in Fig. 1 allows the ratio of the polymer and TiO_2 to be determined. The total amount

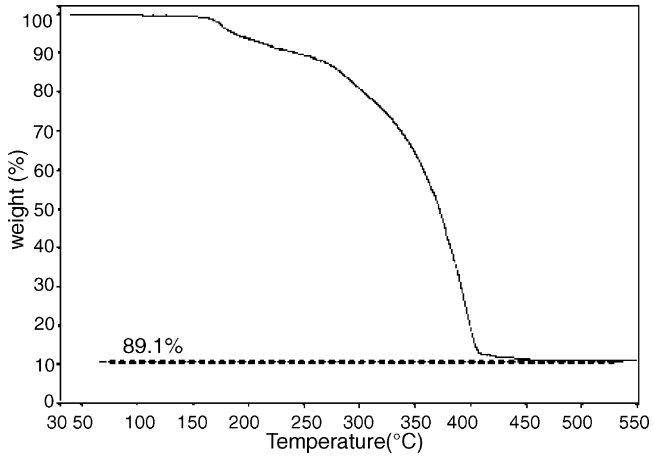

Fig. 1. TGA curve of the raw product consisting of PMMA and Degussa P25 TiO_2 at a heating rate of 10 °C/min under air atmosphere. The polymerization was conducted at the feed concentration of MMA of 11.82 g/l and at TiO_2 concentration of 1 g/l. The sample was obtained after a reaction of 300 min, and the residual concentration of MMA was 2.25 g/l at this time.

of the polymer resulted can be calculate from the data and the amount of TiO_2 added. The polymer yield is defined as the ratio of the amount of polymer and the consumption of monomer. On calculations, it was found that the polymer yield was 85.4%. Similar results can also be obtained in the polymerizations under different conditions [11]. If we take into account the unprecipitated oligomers and an inevitable evaporation of monomer, this polymerization can have very high polymer yield. Therefore, it is clear that the polymerization dominates the photocatalytic reactions of this work.

Fig. 2 gives the GC/MS curve of the upper layer of the suspension mixture. Any traces of the compounds in the bulk solution can be detected. The peak at the retention time of 2.5 min with molecular weight (MW) of 100 g/mol is of course identified as MMA. A new peak with MW of around 110 g/mol appears at the retention time of 8.5 min after this photopolymerization, but it is very weak as observed. This compound may arise from the oxidation of MMA molecules leading to an increase in MW. It is apparent from Fig. 2 that pathway of MMA decomposition is actually limited in our system. Studies on the mechanisms are in progress.

3.1.2. Proof of free radical mechanism

Previously, the studies concerned with the photopolymerizations initiated by semiconductors applied the free radical theory

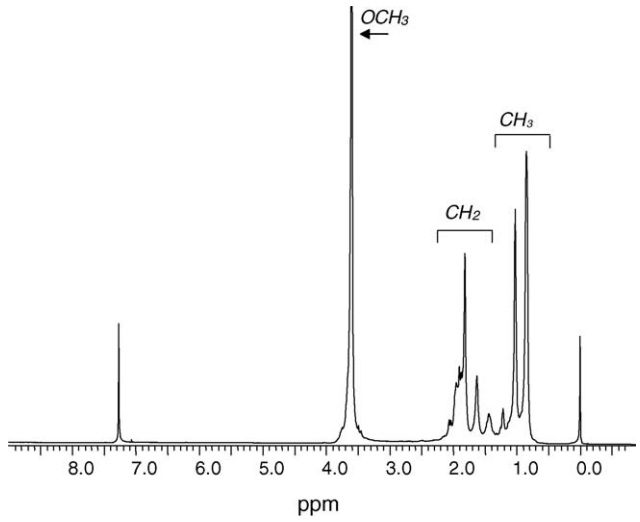

Fig. 3. ^{1}H NMR spectrum of PMMA photopolymerized using by Degussa P25 TiO_2 as initiator at pH 4.5.

Table 1
Stereoregularity of PMMA synthesized

pH	mm%	mr%	rr%
4.6	6.4	37.3	56.3
9.2	6.6	37.7	55.7

for interpretations [5–10], also suggested a probability of ionic chain propagations [5,8]. These polymerizations were carried out in non-aqueous solvents. In the aqueous suspension system of this study, water solvent must inhibit any ionic polymerization because H_2O serves as a highly active transfer-agent to chain propagated ions [16]. Nevertheless, it is impossible for MMA molecules to directly accept the conduction band electrons, deduced from that the reduction potential of band electrons of TiO_2 is about −0.5 V versus NHE [17] while the reduction potential of MMA is about −1.1 V versus NHE [14].

Fig. 3 shows the ^{1}H NMR spectrum of PMMA polymers synthesized this study. Implications of the spectrum include information on the configurational sequences that is governed by the polymerization mechanism. The chemical shift of mm (isotactic), mr (heterotactic) and rr (syndiotactic) sequence is at 0.8, 1.0 and 1.2 ppm, respectively [18]. The polymers obtained are typically of predominant sydiotacty (see Table 1). The sequence ratios depicted in this table are in general characterized by the

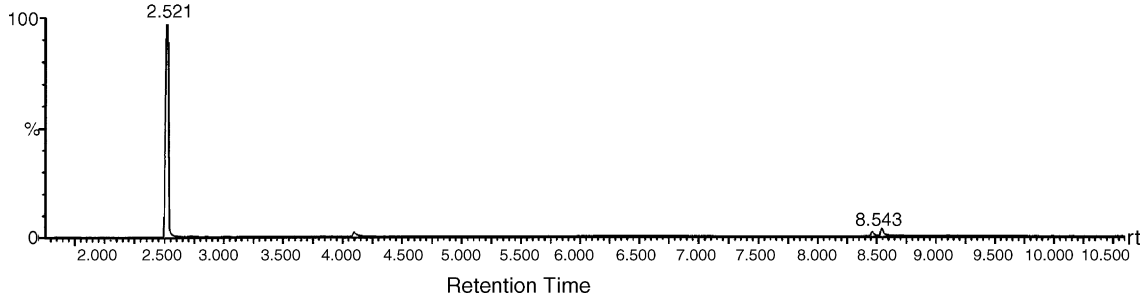

Fig. 2. GC/MS curves of the upper layer of the reacting mixture at a vaporization temperature of 250 °C under a helium stream of 1 ml/min.

free radically prepared PMMA [19]. Accordingly, we conclude that the polymerization of this study indeed follows the free radical mechanism rather than an ionic chain mechanism. The latter was proved to give a considerable higher degree of isotactic structure [20]. The analysis results allow us to apply reliably the free radical kinetics to this photopolymerization.

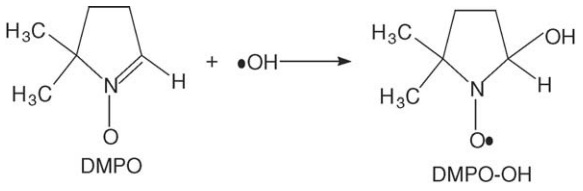

(1)

It was proved that the attack of the photogenerated hole to a MMA molecule produces a monomer radical through abstracting hydrogen from α-methyl [5]. The chain propagation commencing with this primary radical leads to a special terminal β CH_2–CH_2 that distinguishes from other bonds in respect of the thermal cleavage temperature [5,11]. We have detected the production of OH radicals in the P25 TiO_2 suspensions by means of ESR analysis using DMPO as a spin trap. Reaction (1) shows how OH radical to be captured by DMPO molecules. The OH radical rapidly add to nitrone, giving rise to a •DMPO–OH radical that can be detected by the ESR tool [15]. The production of OH radicals under various pH conditions will be involved in Section 3.5.

The active OH radical can also initiate the polymerization of MMA. Likewise, the polymerizations initiated by OH radicals, generated from the photocleavage [21], thermocleavage [22] or redox reaction [16] of H_2O_2, have been extensively reported. The addition of OH radical to MMA gives the monomer radical Reaction (2).

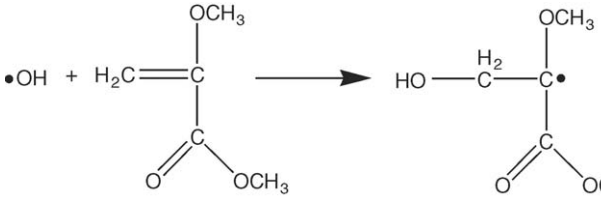

(2)

3.1.3. Surface initiation model

A surface initiation is supposed to take place this study based on the properties of the two initiating species. The hole locates on the surface of semiconductor particles, and it is always unmovable. Since the hole initiation can work via direct hole transfer to MMA in no need of mediations, this reaction necessarily takes place on the surface. OH radical is generated from trapping the primary charge carriers (hole and electron) by the adsorbed reactive species [14]. In literatures, there were numerous contributions suggesting that the reaction of OH radicals with substrates takes place on the TiO_2 surface or in the near solution [15,23,24], though OH radicals are able to escape from the particle. The lifetime of OH radical accounts for this conflict. In view of point that OH radicals can diffuse from the surface of TiO_2 about 100 Å or less into the solution bulk [25], here only the monomer located in the vicinity of a few monolayers of the TiO_2 surface can react with OH radicals. Thus, we simply assume the following reaction sequences:

$$TiO_2 + MMA \rightarrow TiO_2\text{–}MMA \text{ (surface adsorption)} \quad (3)$$

$$TiO_2\text{–}MMA + h\nu \rightarrow TiO_2\text{–}MMA^* \text{(surface initiation)} \quad (4)$$

$$TiO_2\text{–}MMA^* + MMA \rightarrow PMMA \text{ (surface chain propagation)} \quad (5)$$

The rate of photoinitiation R_i is expressed by [16]:

$$R_i = 2\phi I_a \quad (6)$$

where I_a is the adsorbed light intensity, ϕ is the initiation quantum efficiency. The initiation process is the only photochemical step involved in this polymerization. Once the monomer radical is formed, subsequent chain propagations will comply with the known free radical chain mechanism. The rate of polymerization under the steady state approximation is expressed as [16]:

$$\frac{d[M]}{dt} = k_p[M]\left(\frac{R_i}{2k_t}\right)^{1/2} \quad (7)$$

where k_p is the rate constant of chain propagation, k_t is the rate constant of termination. $[M]$ is defined as the concentration of monomer participating into the polymerization. By substituting Eq. (6) into Eq. (7), we obtain:

$$\frac{d[M]}{dt} = k_p k_t^{-1/2}\left(\frac{I_a}{I_0}\right)^{1/2}[M](I_0\phi)^{1/2} \quad (8)$$

where I_0 is the incident light intensity. The value of $k_p/k_t^{1/2}$ is about 0.07 provides that no primary radical-polymer radical termination takes place [26].

3.2. Effect of semiconductor concentration

This polymerization of MMA initiated by Degussa P25 TiO_2 undergoes high conversions (Fig. 4), whereas the monomer conversion measured in absence of TiO_2 is negligible, indicating that the polymerization indeed arises from the photocatalysis of TiO_2. It was observed that this monomer does not absorb the light at 365 nm [11]. This explains why the monomer is avoided from self-polymerization. Taking TiO_2 as the sole absorbent to the irradiation, the absorption ratio, I_a/I_0, of this system is described by the following expression based on Beer–Lambert law [16]:

$$I_a/I_0 = (1 - 10^{-\varepsilon[TiO_2]b}) \quad (9)$$

where ε is the molar absorption efficiency at a given wavelength of the light. b is associated with the dimensions of the reactor. $[TiO_2]$ is the concentration of TiO_2, which is the independent experimental variable in this study. In Eq. (8), I_a/I_0 is the term that actually represents the effect of this variable on the rate of polymerization.

Table 2 shows that I_a/I_0 increases as the concentration of TiO_2 was increased. However, the light absorption changes more

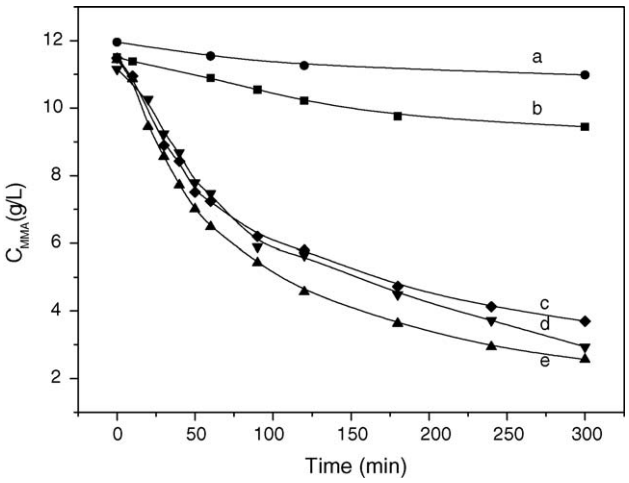

Fig. 4. Profile of MMA concentration during the polymerization initiated by P25 TiO_2 at pH value of 4.5. TiO_2 concentration: (a) 0 (blank experiment); (b) 0.04 g/l; (c) 0.1 g/l; (d) 0.25 g/l; (e) 1 g/l. Light intensity was13.5 mW/cm^2.

Table 2
Light absorption (I_a/I_0) at various concentrations of TiO_2[a]

[TiO_2] (g/l)	0.04	0.1	0.25	1.0	5.0
I_a/I_0	0.649	0.915	0.945	0.954	0.954
$(I_a/I_0)^{0.5}$	0.805	0.957	0.972	0.977	0.977

[a] The wavelength of the light applied was at 365 nm.

slightly as the concentration is increased over 0.1 g/l. From Eq. (9) of Beer–Lambert law, the light absorption is expected to change slowly at high TiO_2 concentrations but must not be saturated theoretically. However, we find experimentally that the absorption is unchanged as TiO_2 concentration exceeds 1.0 g/l. The reason for this phenomenon is not clearly at present, the obstacle of the instrument at the accuracy of 10^{-3} should be taken into account. In the kinetics equation, Eq. (8) rewrote in this work, the effects of the TiO_2 concentration is indirectly inflected by the terms of $(I_a/I_0)^{1/2}$. As R_p is plotted against $(I_a/I_0)^{1/2}$, a straight line is approximately obtained, as shown in Fig. 5. This result basically agrees with the prediction as stated by the kinetics equation.

3.3. Effect of monomer concentration

3.3.1. Diffusion controlled propagation

Provided the polymerization takes place homogeneously, a first-order dependence of the polymerization rate on the monomer concentration will be predicted from Eq. (8). However, the first-order prediction was proved unavailable this study. Taken into consideration that terminations of chain radicals practically make the reaction order slightly deviate from the theoretical prediction, further efforts were paid using the expression of $[M]^n$, where n serves as the adjustable parameter. This function was found also unworkable, indicating a departure from the homogeneous assumption.

Diffusion of small species such as initiator, monomer and primary radical were considered an important aspect of photopolymerizations [3]. In our experiments, the system was adequately

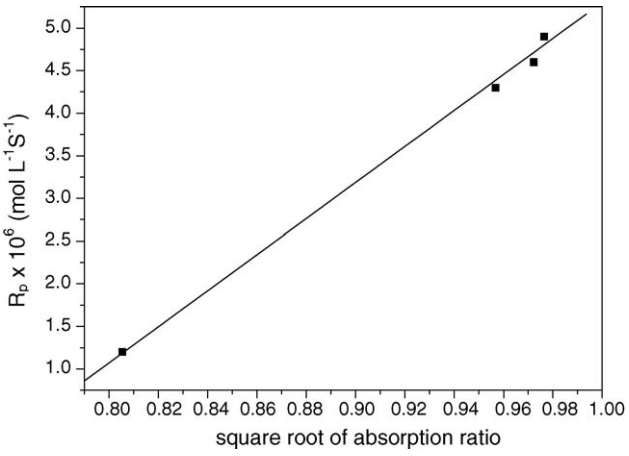

Fig. 5. Dependence of polymerization rate (R_p) on the square root of light absorption ratio (I_a/I_0). MMA concentration was 11×10^{-2} mol/l.

mixed prior to the irradiation. A saturation adsorption at the surface of the nanoparticles can establish before the illumination was switched on. In response to plenty of initiating species at the finite surface of nanoparticles, polymers of high molecular weight can be rapidly built up. Note that the polymeric radicals are less mobile. For MMA polymerizations in aqueous system, the chain transfer to monomer or to solvent was ignored on basis of low chain-transfer coefficients [16,26]. Thus, the chain propagation is unlikely to occur in the solution bulk. In our previous work [11], the morphology of TiO_2 nanoparticles encircled by the photogenerated PMMA was observed. With these in mind, we suppose that the chain propagation continues at the surface Reaction (5) after the surface initiation. The polymerization can proceed with MMA diffusing continuously onto the nanoparticles. The driving force is the concentration gradient because the propagation makes the concentration of the free monomer around the surface lower than the bulk of solution.

At the steady state, mass equilibrium is supposed to establish between the monomer diffusion and the consumption, i.e. the rate of chain propagation equals the diffusion flux. Fick's first law defines the diffusion flux as [27]:

$$J = DS\frac{\mathrm{d}[M]}{\mathrm{d}x} \tag{10}$$

where $\mathrm{d}[M]/\mathrm{d}x$ is the concentration gradient on each side of the diffusion surface S. The diffusion coefficient D is known to be concentration dependent [28], which is often expressed by an exponential function as follows:

$$D = D_0 \exp(\xi[M]_b) \tag{11}$$

$[M]_b$ is the concentration of monomer in the solution bulk, which equals the feed concentration if the adsorbed amount is ignored. Thus, we obtain:

$$R_p = D_0 S \exp(\xi[M]_b)\frac{\Delta M}{\Delta x} \tag{12}$$

We connect the data of R_p to the feed concentration of monomer using Eq. (12). The results depicted in Fig. 6 indicate that the

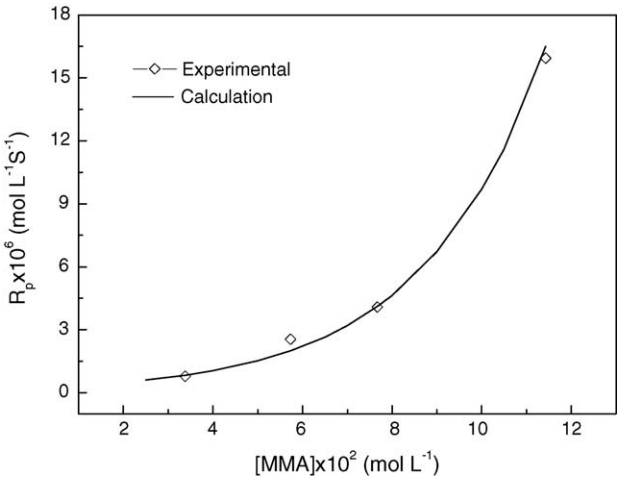

Fig. 6. Comparisons of the experimentally measured polymerization rate (◊) with the predictions (—) calculated on Eq. (13) at various MMA feed concentrations. TiO_2 concentration was 1 g/l. The light intensity was13.5 mW/cm^2.

experimental R_p well agree with the following simulated expression:

$$R_p = 0.24 \exp(0.37 \times 10^2 [M]_b) \quad (13)$$

This result not only indicates the exclusive match of the exponential function, but also support that mass diffusion is really involved in the polymerization of this study. The diffusion towards surface is always forced by the concentration gradient to compensate for the monomer consumption, no matter the chain radicals can instantly capture the diffused monomer or not. The rate of propagation only depends on MMA concentration around the surface and thus the diffusivity of the monomer.

3.3.2. Influence on molecular weight

It was found that the number-averaged molecular weight ($\bar{M}_n$) of the polymer increase rapidly with increasing the monomer feed concentration (Table 3). As the concentration was increased from 3.4 to 11.4 g/l, $\bar{M}_n$ was increased by almost 50 times. This trend differs from the ideally linear increase predicted from the first-order kinetics as follows. It is known that the kinetic chain length, which is in proportional to the number-average degree of polymerization ($\bar{X}_n$), equals R_p/R_i under the steady state approximation [16]. At given light intensity and content of semiconductor, R_i is taken as constant. In the case of the first-order reaction, $\bar{M}_n$ should increase linearly with the concentration of monomer at the ideal steady-state. With the aid of above relations, the observed exponential dependence of R_p on the feed concentration explains the trend of $\bar{M}_n$ this study, verifying the critical effects of diffusion controlled propagation.

Table 3
$\bar{M}_n$ and dispersity of the polymer obtained at various concentrations of monomer

[MMA] (g/l)	3.4	5.7	7.7	11.4
$\bar{M}_n \times 10^{-4}$ (g/mol)	0.17	0.59	4.62	8.58
Dispersity	5.40	3.70	2.02	2.73

The reaction was carried out for 300 min. [TiO_2] = 1.0 g/l, [I_0] = 13.5 mW/cm^2.

3.4. Effect of incident light intensity

The initiation quantum efficiency (ϕ), which is of great value in photoinitiated polymerizations, can be calculated through the following expression [29]:

$$\phi = \frac{\phi_p}{\bar{X}_n} \quad (14)$$

where ϕ_p is defined as the ratio of the number of monomer molecules initiated to the number of photons absorbed. $\bar{X}_n$ is the average degree of polymerization.

$$\phi = \frac{(C_i - C_e) \times V}{\bar{M}_n \times N_{abs}} \quad (15)$$

where C_i is the initial concentration of monomer (g/l), C_e is the concentration of monomer remained after reaction (g/l), V is the volume of the reacting system, N_{abs} is number of the photons absorbed by TiO_2. It was calculated out that the quantum efficiency ranges 10×10^{-4} to 25×10^{-4}, as shown in Fig. 7. The quantum efficiency was found to decrease with increasing the incident light intensity, which is involved in the association of the light intensity versus the recombination of electron–hole pairs.

We would like to discuss the theoretical effects of chain-transfer reactions on the value of ϕ calculated in Eq. (14), although this equation has been frequently employed in relevant literatures. During radical polymerizations, the radicals can transfer to monomer, solvent and polymer. The chain-reaction to either monomer or solvent should make the calculated value of ϕ higher than the theoretical value, whereas the chain-reaction to polymer shows no influence. In the case of MMA polymerizations in aqueous system, the chain transfer to monomer or to water solvent was usually ignored because of the low chain-transfer coefficients [16,26]. Thus, the calculated value of ϕ here is believed to close to its theoretical value.

Previous predictions of a $\phi \propto I_a^{-1/2}$ dependence at $\phi \leq 1$ were made on basis of the association of second-order kinetics

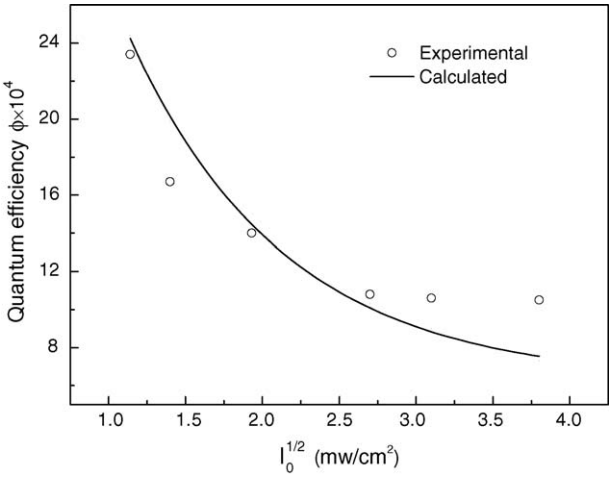

Fig. 7. Initiation quantum efficiency (ϕ) as a function of the square root of incident light intensity. TiO_2 concentration was 1 g/l. MMA concentration was 11×10^{-2} mol/l, pH 4.5.

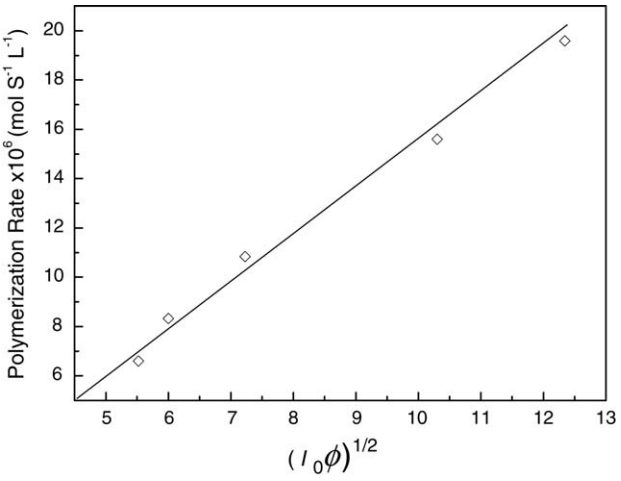

Fig. 8. Dependence of polymerization rate (R_p) on the square root of $I_0\phi$. TiO_2 concentration was 1 g/l. TiO_2 concentration was 1 g/l. MMA concentration was 11×10^{-2} mol/l, pH 4.5.

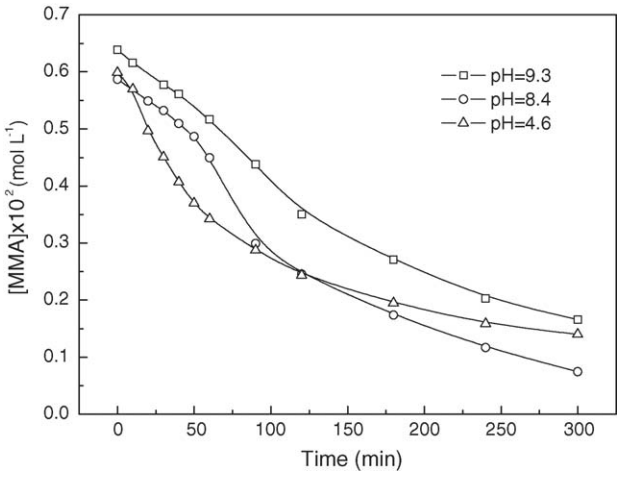

Fig. 9. Influences of pH on MMA polymerization initiated by Degussa p25 TiO_2. TiO_2 concentration was 1 g/l. The light intensity was 13.5 mW/cm^2.

with bimolecular single carrier pair recombination [23]. Implications of the simulated plot of ϕ versus $I_a^{-1/2}$ in Fig. 5 show that such a scenario approximately applies to our polymerization. Ollis [30] stated that the dependence power of $-1/2$ applies to the cases where intermediate I_0 was employed in photomineralizations of organics.

R_p is found to decreases with increasing the light intensity, while the values of $I_0\phi$ show a similar trend. In Fig. 8 showing R_p against $(I_0\phi)^{1/2}$ at a fixed concentration of TiO_2, a straight line is observed. Considering that the value of I_a/I_0 keeps constant at a given concentration of TiO_2, this result agrees with the theoretical prediction as stated by Eq. (8). If R_p is independently connected with I_0, a $R_p \propto I_0^{1/2}$ dependence is infeasible unlike the polymerizations with organic photo-sensitizers, in which ϕ only depends on the chemical nature of the initiators at given wavelength of UV light. Here, ϕ is a function of the light intensity that rather serves as an independent experimental variable. The proven match of Eq. (8) suggests that the association of R_p versus $I_0\phi$ is a sound alternative to investigating the effects of light intensity. The physical meaning of $I_0\phi$ is understood as the effective light intensity applied to the polymerization system.

Table 4 shows that $\bar{M}_n$ increase as the incident light intensity was increased. This trend is actually governed by the polymerization kinetics, and can be interpreted in terms of the kinetic chain length described earlier. Considering the relation of $R_p \propto (I_0\phi)^{1/2}$, R_p dividing by the rate of initiation ($R_i = 2\phi I_a$) gives that the kinetic chain length is in inverse proportional to $(I_0\phi)^{1/2}$ at given concentration of semiconductors. This dependence explains the observed decrease in $\bar{M}_n$.

Table 4
$\bar{M}_n$ and dispersity of PMMA obtained at various incident light intensities

$[I_0]$ (mW/cm^2)	1.3	2.0	3.7	7.3	10.0	14.5
$\bar{M}_n \times 10^{-4}$ (g/mol)	13.2	13.9	11.1	10.3	8.1	6.1
Dispersity	2.86	3.14	3.23	2.63	2.72	2.85

The reaction was carried out for 300 min. $[TiO_2] = 1.0$ (g/l); $[MMA] = 12 \times 10^{-2}$ mol/l.

3.5. Effects of pH condition

3.5.1. Influence on the rate of polymerization

In the case of Degussa P25 TiO_2, the pH of zero point of charge, pH_{zpc} 6.25 [14]. Fig. 9 shows the polymerization curves under pH conditions on each side of pH_{zpc}. It is important to find that, from slopes of the plots, the rate of polymerization at low degree of conversion varies depending on the pH values. The rate of polymerization at the condition of $pH < pH_{zpc}$ is twice as high as that at $pH > pH_{zpc}$. It is noteworthy that obvious aggregations of TiO_2 were not observed under the pH conditions of this work.

As depicted in Table 1, the stereoregularity of the polymers remains unchanged irrespective of pH. Therefore, this polymerization consistently follows the free radical chain mechanism no matter whether the pH is above or below pH_{zpc}. These experiments were conducted under the same conditions of the incident light intensity, monomer concentration and dosage of TiO_2. Also, the absorbed light intensity was determined to be almost uninfluenced with the pH variations. From Eq. (8), it follows that the initiation quantum efficiency of this polymerization is pH dependent.

Changing pH of this system can vary the surface electrostatic property of P25 TiO_2 [31]. However, we consider that MMA adsorption onto TiO_2 would not be a function of the surface state, owing to the electroneutrality of MMA. Initiating MMA direct via the holes is most likely to be uninfluenced with pH values. On contrary, the properties of OH radicals should be taken into account.

Fig. 10 gives the ESR spectrum of OH radicals trapped by DMPO molecules under the pH conditions on each side of pH_{zpc} of TiO_2. The spectrum is typical quadruple peaks of OH-DMPO Reaction (1) [15]. Its high symmetry implies that the yields of other radicals are negligible. As observed in Fig. 10, the production of OH radicals is strongly pH dependent. The yield measured at the condition of $pH > pH_{zpc}$ is

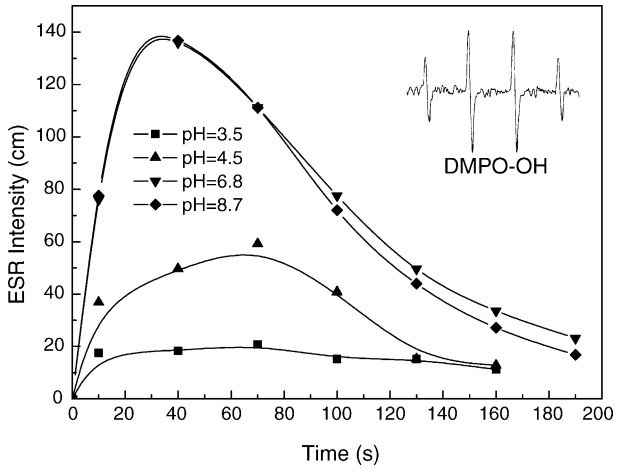

Fig. 10. pH dependent yields of DMPO–OH radicals determined by ESR analysis. The ESR spin-trapping experiments were conducted with the TiO_2 aqueous suspension containing 0.04 g/l TiO_2 and 100 mmol/l DMPO. The intensity of UV light at 365 nm was 0.56 mW/cm^2.

about twice more than that at $pH < pH_{zpc}$. This result implies that the pH dependent production of OH radicals is critical to the observed pH dependence of polymerization rate. Thus, it is necessary to discuss the pathways to OH radicals in our experiments.

3.5.2. Discussions on pH influences on the initiating species

The system of this study was not degassed purposely. With a JPB-607 Oxygen-meter, the saturation concentration of oxygen dissolved in the system was measured to be 8.2 mg/l, as the same as the data elsewhere. Adsorptive oxygen at the surface of particle is electron trapper. The formation of $HO_2^\bullet$ radicals from O_2^- and H^+, giving rise to H_2O_2 was proposed as one way of producing OH radical [14]:

$$O_2\,(\text{ads}) + e^- \rightarrow O_2^{\bullet -} \quad (16)$$

$$O_2^{\bullet -} + H^+ \rightarrow HO_2^\bullet \quad (17)$$

$$2HO_2^\bullet \rightarrow H_2O_2 + O_2 \quad (18)$$

$$H_2O_2 + O_2^- \rightarrow OH^\bullet + OH^- + O_2 \quad (19)$$

This reaction can proceed in the reverse direction once the pH is higher than pK_a (4.88) for $HO_2^\bullet$ radical [32]. Also, another contributor [33] suggested that this pathway to OH radical would be depressed on increasing the pH. Here, the opposite trend is actually observed. This phenomenon strongly indicates another way predominating over the production of OH radical at the increased pH this study.

Producing OH radical via trapping the hole should be taken into accounts [34]:

$$H_2O\,(\text{ads}) + h_{vb}^+ \rightarrow OH^\bullet + H^+ \quad (20)$$

$$OH^- + h_{vb}{}^+ \rightarrow OH^\bullet \quad (21)$$

The reaction of trapping holes by H_2O is pH independent. Importantly, the photoproduced holes can directly oxidize absorbed OH^- at the semiconductor surface to OH radicals Reaction (21). In our experiments, the pH value of the system was adjusted by adding a sodium hydroxide solution, which actually supplies lots of OH^- ions. It, therefore, is sound to ascribe the observed increases in OH yields at the increased pH to a sharp increase in the number of OH^- ions. Similarly, several investigators [33,35,36] have explained their pH-relevant findings in terms of the dependence of OH radical on the number of OH^- ions at the surface of TiO_2. The results of this study, with aids of the results from ESR analysis, suggest further that trapping photogenerated holes by OH^- is a very competitive pathway towards OH radical in aqueous systems.

The yield of OH radical is expected to be larger in case of pH 8.7 than pH 6.8 because more OH^- can be supplied. However, only the $^\bullet$DMPO–OH radical, resulting from the addition reaction of OH radical and DMPO, was detected by the ESR tool. In the analysis, the addition reaction is in competition with the termination reaction between OH radical radicals. The termination reaction makes OH radical disappear, and its rate may also be intensified with an increase in the concentration of OH radical. The termination of OH radical radicals would account for why there is no obvious difference between pH 6.8 and 8.7 cases in Fig. 10.

By using picosecond and nanosecond laser photolysis to excite colloidal TiO_2 particles of 6 nm radius in aqueous, Rothenberger [37] monitored the dynamics of charge carrier trapping in this semiconductor material. They found that the trapping of conduction band electrons was a very rapid process occurring with the leading edge of the 30-ps laser flash. The trapping of the valence band hole, presumable by surface OH^- groups, was much slower process requiring an average time of 250 ns. The dynamics results would explain why the trapping of hole by OH^- groups become dominant once a sodium hydroxide solution is added in this study, assuming that the trapping processes are controlled by mass diffusion of the absorptive trappers. The long-lived holes seem ready to react with the diffused OH^- groups.

Back to the pH dependent initiation quantum efficiency of interest, both $h_{vb}{}^+$ and OH radical can work as initiators of the polymerization, and the two initiators should compete one another. At the increased pH over pH_{zpc}, the initiation reaction by the photogenerated hole would be weakened because a number of holes participate into the parallel reaction of oxidizing OH^- and perhaps H_2O, while the initiation of OH radicals is intensified because the number of OH radicals is increased. Assuming that the hole is more ready to react with the monomer than OH radicals, the higher initiation quantum efficiency, and thus the observed higher polymerization rate at the higher pH can be explained.

On the other hand, a notable difference in the termination of radicals between the hole and OH radical initiations should be taken into account. In the case of OH radical, the monomer radicals or the chain radicals are necessarily terminated by the primary radicals (OH radical), in addition to other kinds of radicals. Differently, the hole cannot directly terminate these radical. Thus, this also devotes a higher initiation quantum efficiency to the hole initiation.

4. Conclusions

The kinetics of the photopolymerization of methyl methacrylate initiated by TiO_2 nanoparticles are studied with the aim of obtaining a better understanding of this polymerization, and thus acquiring a knowledge of controlling the polymerization and the structures of the synthesized polymers. This polymerization follows the free radical chain mechanism, along with the dependences of polymerization rate on the TiO_2 concentration and the incident light intensity complying with the predictions stated by the kinetics equation. The rapid increase in polymerization rate with increasing concentration of methyl methacrylate is explained by introducing a surface chain propagation model. The effect of mass transfer is incorporated through addition of a diffusion flux term to the mass equilibrium of monomer. The initiation quantum efficiency is found to decrease with increasing incident light intensity.

The rate of polymerization is pH dependent, while the polymer configuration remains unchanged. Our results from ESR spin-trapping experiments at various pH conditions suggest that trapping holes by OH^- act as a competitive way towards OH radical. With aids of these results, pH dependence of the initiation quantum efficiency is correlated to the influences of pH on the initiating species.

Acknowledgments

This research is supported by National Natural Science Fund of China. Financial support from Shanghai Nanotechnology Promotion Center (SNPC) is gratefully acknowledged.

References

[1] J.V. Crivello, J.L. Lee, J. Polym. Sci. Part A 28 (1990) 479–503.
[2] C.M. Previtali, S.G. Bertolotti, M.G. Neumann, I.A. Paster, A.M. Rufs, M.V. Encinas, Macromolecules 27 (1994) 7454–7458.
[3] T.M. Lovestead, A.K. O'Brien, C.N. Bowman, J. Photochem. Photobiol. A: Chem. 159 (2003) 135–143.
[4] I.G. Popovic, L. Katslkas, H. Weller, Polym. Bull. 32 (5–6) (1994) 597–603.
[5] I.G. Popovic, L. Katslkas, U. Muller, J.S. Velickovic, H. Weller, Macromol. Chem. Phys. 195 (3) (1994) 889–904.
[6] B. Kraeutler, H. Reiche, A. Bard, J. Sci. Polym. Lett. 17 (1979) 535–540.
[7] A.J. Hoffman, G. Mills, H. Yee, M.R. Hoffman, J. Phys. Chem. 96 (1992) 5546–5552.
[8] A.J. Hoffman, G. Mills, H. Yee, M.R. Hoffman, J. Phys. Chem. 96 (1992) 5540–5546.
[9] Z.Y. Huang, T. Barber, G. Mills, M.B. Morris, J. Phys. Chem. 98 (1994) 12746–12752.
[10] A.L. Stroyuk, V.M. Granchak, A.V. Korzhak, S.Ya. Kuchmii, J. Photochem. Photobiol. A: Chem. 162 (2004) 339–351.
[11] X.Y. Ni, C. Dong, J. Macromol. Sci., A: Pure Appl. Chem. 41A (2004) 547–563.
[12] J.O. McCaldin, Prog. Solid State Chem. 26 (1998) 241–265.
[13] R. Asahi, T. Morikawa, T. Ohwaki, K. Aoki, Y. Taga, Science 293 (2001) 269–271.
[14] M.R. Hoffman, S.T. Martin, W. Choi, D.W. Bahnemann, Chem. Rev. 95 (1995) 69–96.
[15] M.A. Grela, M.E.J. Coronel, A.J. Colussi, J. Phys. Chem. 100 (1996) 16940–16946.
[16] G. Odian, Principles of Polymerization, third ed., Wiley-Interscience, 1991.
[17] P.V. Kamat, Chem. Rev. 93 (1993) 267–300.
[18] L. Dong, J.T. Hill, J.H. O'Donnell, T.G. Carwell-pomerantz, P.J. Pometry, A.K. Whittaker, K. Hatada, Macromolecules 28 (1995) 3681–3691.
[19] J. Suarez, E. Mano, E. Monterio, M. Tavares, J. Appl. Polym. Sci. 85 (2002) 886–895.
[20] E. Ihara, T. Tsuyoshi, I. Kenzo, J. Polym. Sci., Part A: Polym. Chem. 41 (2003) 1962–1977.
[21] B. Gilmene, G.H. Marcelo, J. Photochem. Photobiol. A: Chem. 149 (2002) 115–119.
[22] J.L. Pradel, B. Boutevin, B. Ameduri, J. Polym. Sci., Part A: Polym. Chem. 38 (2000) 3293–3302.
[23] D.F. Ollis, H. Al-Ekabi (Eds.), Photocatalysis Purification and Treatment of Water and Air, Elsevier, Amsterdam, 1993.
[24] G.R. Helz, R.G. Zepp, D.G. Crosby (Eds.), Aquatic and Surface Photochemistry, CRC, Boca Raton, FL, 1994.
[25] C.S. Turchi, D.F. Ollis, J. Catal. 122 (1990) 178–192.
[26] C.H. Bamford, W.G. Bard, A.R. Taylor, The Kinetics of Vinyl Polymerization by Radical Mechanism, Butterworths, London, 1958.
[27] J. Crank, The Mathematic of Diffusion, Clarendon Press, Oxford, 1986.
[28] J.B. Brun, C. Larchet, G. Bulvestre, B. Auchair, J. Membr. Sci. 25 (1985) 55–100.
[29] M.R. Rodrigues, F. Catalina, M.G. Neumann, J. Photochem. Photobiol. A: Chem. 127 (1999) 147–152.
[30] D.F. Ollis, E. Pelizzetti, N. Serpone, Environ. Sci. Technol. 25 (1991) 1522–1529.
[31] V. Brezova, A. Stasko, S. Biskupie, A. Blazkova, B. Havlinova, J. Phys. Chem. 98 (1994) 8977–8984.
[32] K.H. Wang, Y.H. Hsieh, C.H. Wu, C.Y. Chang, Chemosphere 40 (2000) 389–394.
[33] J.C. D'Olivera, G. Al-Sayyed, P. Pichat, Environ. Sci. Technol. 24 (1990) 990–996.
[34] K. Okamoto, Y. Yamamoto, H. Tanaka, M. Hanaka, A. Itaya, Bull. Chem. Soc. Jpn. 58 (1985) 2023–2028.
[35] T. Wei, C. Wan, J. Photochem. Photobiol. A: Chem. 69 (1992) 241–249.
[36] W.H. Leng, H. Liu, S.A. Cheng, J.Q. Zhang, C. Cao, J. Photochem. Photobiol. A: Chem. 131 (2000) 125–132.
[37] G. Rothenberger, J. Moser, M. Gratzl, N. Serpone, D.K. Sharma, J. Am. Chem. Soc. 107 (1985) 8054–8059.